

Absorptive Bandstop Filter With Prescribed Negative Group Delay and Bandwidth

Liang-Feng Qiu, *Student Member, IEEE*, Lin-Sheng Wu, *Senior Member, IEEE*,
Wen-Yan Yin, *Fellow, IEEE*, and Jun-Fa Mao, *Fellow, IEEE*

Abstract—An absorptive bandstop filter is proposed and synthesized with prescribed negative group delay (NGD) and negative group delay bandwidth (NBW). It is realized with resistor-loaded coupled-line structures where the NGD can be controlled by the Q -factors of resonators. The resistor of the first section is determined for impedance matching, also providing a negative delay. A prototype is developed, following the proposed design procedure, with $\text{NGD} = -6.5$ ns and $\text{NBW} = 105$ MHz obtained. The proposed method is experimentally validated by the good agreement between the synthesized and measured results.

Index Terms—Absorptive bandstop filter, coupled microstrip line, negative group delay (NGD), resistor loading.

I. INTRODUCTION

IN recent years, networks with negative group delay (NGD) have drawn much attention, due to their potential applications in communication systems, such as feedforward linearization amplifiers, antenna array systems, phase shifters, and power dividers. The NGD phenomenon can be observed within a limited frequency band of signal attenuation through certain media where the amplitude envelope of a signal is transmitted in advance of the undergoing delay [1], [2]. The low-frequency NGD circuits are realized by using series or shunt RLC resonators. Then, the distributed transmission line resonators are utilized in the microwave regime [3]–[7]. The conventional NGD circuits suffer from high in-band attenuation, poor NGD or magnitude flatness, and narrow negative group delay bandwidth (NBW). Attempting to overcome some of these issues, different methods have been presented. In [4] and [5], cross-coupled topologies are utilized to reduce the attenuation. In [6], the transversal filter is synthesized to improve the NGD flatness. In [7], reflective bandstop filters (BSFs) are designed with enhanced NBW, where an additional impedance transformer is required to obtain good in-band matching. However, the impedance transformer changes the reference impedance of the NGD BSF, and decreases the NGD and NBW. Therefore, careful tuning should

Manuscript received January 17, 2017; accepted April 25, 2017. Date of publication June 20, 2017; date of current version July 3, 2017. This work was supported by the National Science Foundation of China under Grant 61370008 and Grant 61361166010. (Corresponding author: Liang-Feng Qiu.)

L.-F. Qiu, L.-S. Wu, and J.-F. Mao are with the Key Laboratory of Ministry of Education of Design and Electromagnetic Compatibility of High-Speed Electronic Systems, Shanghai Jiao Tong University, Shanghai 200240, China (e-mail: wallish@sjtu.edu.cn).

W.-Y. Yin is with the Key Laboratory of Ministry of Education of Design and Electromagnetic Compatibility of High-Speed Electronic Systems, Shanghai Jiao Tong University, Shanghai, 200240 China, and also with the School of Information Science and Electronic Engineering, Zhejiang University, Hangzhou 310058, China (e-mail: wyyin@zju.edu.cn).

Color versions of one or more of the figures in this paper are available online at <http://ieeexplore.ieee.org>.

Digital Object Identifier 10.1109/LMWC.2017.2711572

1531-1309 © 2017 IEEE. Personal use is permitted, but republication/redistribution requires IEEE permission.
See http://www.ieee.org/publications_standards/publications/rights/index.html for more information.

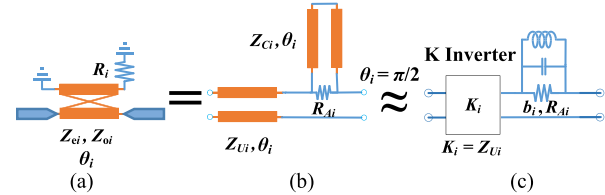


Fig. 1. (a) Coupled-line section of the proposed BSF filter; (b) its equivalent transmission line model; and (c) its approximated circuit model.

be further carried out for the matched filter to satisfy the design specifications.

In this paper, an absorptive BSF with prescribed NGD is proposed. It is built up with resistor-loaded coupled-line structures, and the parameters are synthesized directly. The resistors are used to control the resonator Q -factors and absorption. Thus, the changing of reference impedance and NGD, introduced by the transformer, is avoided, and good return loss (RL) is obtained.

II. THEORY AND DESIGN EQUATION

Fig. 1(a) shows a coupled-line section of the proposed BSF, and its equivalent transmission line model is shown in Fig. 1(b). By making the Y -parameters of Fig. 1(a) and (b) equal to each other, the element values in Fig. 1(b) are obtained as

$$Z_{Ui} = \frac{2Z_{ei}Z_{oi}}{Z_{ei} + Z_{oi}}, Z_{Ci} = \frac{(Z_{ei} - Z_{oi})^2}{2(Z_{ei} + Z_{oi})}, R_{Ai} = R_i \left(\frac{Z_{ei} - Z_{oi}}{Z_{ei} + Z_{oi}} \right)^2. \quad (1)$$

The transmission line model can further be approximated by the circuit in Fig. 1(c) when the electrical length $\theta_i = \pi/2$. Here, the unit element is regarded as a K -inverter, and the resistor-loaded $\lambda/4$ shorted stub is regarded as a lossy parallel resonant circuit. The susceptance slope parameter and the unloaded Q -factor of the resonator are derived as

$$b_i = \pi/4Z_{Ci}, \quad Q_i = b_i R_{Ai} = \pi R_i / (2Z_{ei} + 2Z_{oi}). \quad (2)$$

Based on the above analysis, the proposed BSF in Fig. 2(a) can be represented by the circuit model in Fig. 2(b). It is a traditional BSF when the resistors are removed. So when setting all the inverter impedances to $K_i = Z_{Ui} = Z_0$ except the first one, (3) can be obtained, similar to that in [8]

$$Z_{U1} = Z_0 \sqrt{m_1 / (g_0 g_1)}, \quad Z_{Ci} = \pi Z_0 \text{FBW} m_i / 4 \\ m_N = g_N g_{N+1} \text{ and } m_i = g_i g_{i+1} / m_{i+1} \text{ for } i = 1 \cdots N - 1 \quad (3)$$

where FBW is the fractional bandwidth, and g_i is the element value of a low-pass prototype. Then, the even- and odd-mode impedances are calculated from (1) as

$$Z_{oi} = \frac{Z_{Ui}}{1 + \sqrt{Z_{Ci} / (Z_{Ci} + Z_{Ui})}}, \quad Z_{ei} = \frac{Z_{Ui}}{1 - \sqrt{Z_{Ci} / (Z_{Ci} + Z_{Ui})}}. \quad (4)$$

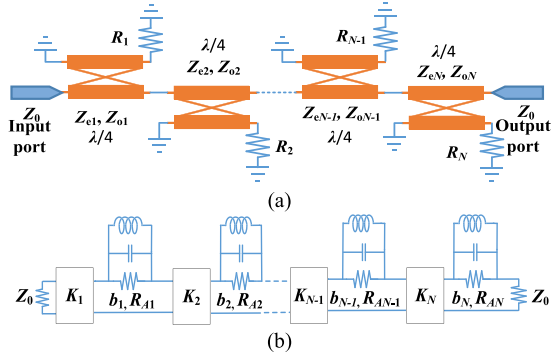


Fig. 2. (a) Proposed absorptive BSF topology and (b) its equivalent circuit model.

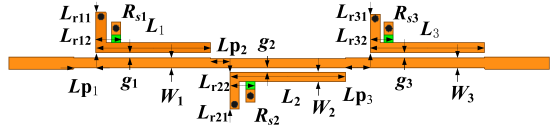


Fig. 3. Layout of the fabricated BSF with NGD. Geometrical parameters are $L_1 = L_3 = 17.8$, $W_1 = W_3 = 1.55$, $g_1 = g_3 = 0.32$, $L_{p1} = 3.5$, $L_{r11} = 6.23$, $L_{r12} = 3.8$, $L_2 = 18$, $W_2 = 1.41$, $g_2 = 0.22$, $L_{p2} = 3$, $L_{r21} = 5.62$, $L_{r22} = 3.9$, $L_{p3} = 3.8$, $L_{r31} = 5.94$, $L_{r32} = 3.6$ (unit: mm). The resistances are $R_{s1} = 110 \Omega$, $R_{s2} = 620 \Omega$, and $R_{s3} = 680 \Omega$.

When the i th resonator is referenced to the impedances Z_{Li} and Z_{Ri} for its left and right sides, respectively, its related transmission coefficient S_{21i} can be obtained as

$$S_{21i} = \frac{2\sqrt{Z_{Li}Z_{Ri}}[R_{Ai}^{-1} + j(\omega C_i - \omega^{-1}L_i^{-1})]}{(Z_{Li} + Z_{Ri})[R_{Ai}^{-1} + j(\omega C_i - \omega^{-1}L_i^{-1})] + 1}. \quad (5)$$

Then, the NGD at the central frequency ω_0 is calculated by

$$\tau_i = -\left. \frac{d\angle S_{21i}}{d\omega} \right|_{\omega=\omega_0} = \frac{-2R_{Ai}^2 b_i}{\omega_0(R_{Ai} + Z_{Li} + Z_{Ri})}. \quad (6)$$

From (1) and (6), the relation between R_i and τ_i is derived by

$$R_i = -\frac{\omega_0 \tau_i}{4b_i} \left(1 + \sqrt{1 - \frac{8(Z_{Li} + Z_{Ri})b_i}{\omega_0 \tau_i}} \right) \left(\frac{Z_{ei} + Z_{oi}}{Z_{ei} - Z_{oi}} \right)^2. \quad (7)$$

The first resistor is designed to match the lossy filter with the input port when resonating, and it can be derived as

$$R_1 = R_{A1} \left(\frac{Z_{e1} + Z_{o1}}{Z_{e1} - Z_{o1}} \right)^2 = \frac{4 - Z_0 Z_{in1} (1/Z_{e1} + 1/Z_{o1})^2}{Z_0 (1/Z_{o1} - 1/Z_{e1})^2} \quad (8)$$

where Z_{in1} is the input impedance of the rest part of filter seen from the right side of the first coupled-line section at ω_0 . Note that the parasitic capacitance of lumped resistors will shift the resonant frequencies, if the susceptance slope parameter of the resonator seen from the location of resistor is relatively small. In order to reduce the effect, the resistors are mounted close to the shorted ends of resonators, as shown in Fig. 3. R_{si} is selected to make the Q -factor equal to the calculated one from (2), that is

$$Q_i^{-1} \approx Q_{Rsi}^{-1} + Q_{i0}^{-1}, \quad Q_{Rsi} \approx \pi R_{si} / [2(Z_{ei} + Z_{oi}) \sin^2 \theta_{si}] \quad (9)$$

where θ_{si} is the electrical length from the resistor to the shorted end of the i th resonator, and Q_{i0} is the Q -factor of i th resonator without loading resistors. Then, the resistance R_{si} is obtained as

$$R_{si} \approx \frac{2(Z_{ei} + Z_{oi}) \sin^2 \theta_{si}}{\pi(1/Q_i - 1/Q_{i0})}, \quad \theta_{si} \gg \arctan \frac{(Z_{ei} + Z_{oi})}{2R_i}. \quad (10)$$

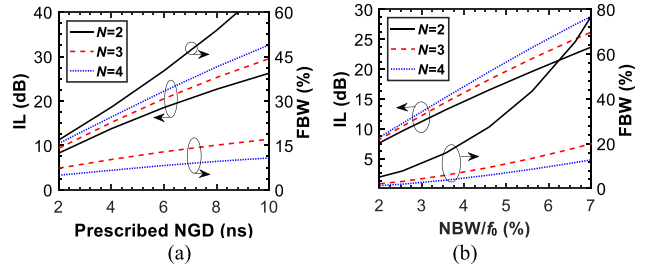


Fig. 4. IL and required FBW versus: (a) prescribed NGD and the filter order N when $\text{NBW} = 110 \text{ MHz}$ and $f_0 = 1.962 \text{ GHz}$; (b) prescribed NBW/f_0 and the filter order N when $\tau_{total} = -6.5 \text{ ns}$ and $f_0 = 1.962 \text{ GHz}$.

The constraint of θ_{si} in (10) is obtained by comparing the Y -parameters of the coupled-line sections in Figs. 1(a) and 3 at ω_0 . The responses of the filter will be slightly deteriorated with decreasing θ_{si} . So θ_{si} should be selected properly.

Set all delay τ_i of the i th resonator ($i = 2$ to N) equal to the predefined section delay τ_C with $Z_{Li} = Z_{Ri} = Z_0$ assumed, and the total delay of the proposed BSF is approximated by [7]

$$\tau_{total} \approx a\tau_C + b \quad (11)$$

where a is the correction factor to take into account the fact that the reference impedances of resonators working in the filter are different from Z_0 , leading to the individual group delay τ_i different from τ_C , and b is a constant value to count for the delay introduced by the first resonator and the K -inverters. The value of a is mainly determined by the filter order N and FBW, and it can be obtained through the curve-fitting method as

$$a \approx (N - P_1) \left(\frac{P_2}{P_3 + \text{FBW}} + P_4 \right) \quad (12)$$

where $P_1 = 0.964$, $P_2 = 0.024$, $P_3 = 0.039$, and $P_4 = 0.97$ are obtained for the Chebyshev filter. Note that $b = 0$ is used as an initial value since b is much smaller than τ_{total} and the exact value of a and b will be updated during the subsequent design procedure.

The IL and required FBW are shown in Fig. 4(a) as the functions of prescribed NGD, with $f_0 = 1.962 \text{ GHz}$, $\text{NBW} = 110 \text{ MHz}$, and $N = 2, 3$, and 4 . They are also shown in Fig. 4(b) versus NBW/f_0 when $\tau_{total} = -6.5 \text{ ns}$. It is seen that when NGD or NBW increases, both IL and FBW increase. So, there is a tradeoff among NGD, IL, and NBW. The IL increases with increasing N , and hence, lower order filters are preferred but with higher FBW required, which may lead to unrealizable filter topology, especially for $N = 2$.

Compared to the unmatched third-order NGD BSF, i.e., R_1 are also from (6), the NBW of the matched filter are almost the same. However, the 60-MHz NBW of matched filter in [7] is much smaller than that of the unmatched one, as shown in Fig. 5(a), where the resistances are tuned to achieve the same NGD of -6.5 ns . The proposed matched filter provides the IL of 12.2 dB, 8 dB lower than that in [7]. The worst RL within the NGD band is improved by 20 dB, as shown in Fig. 5(b).

For the prescribed f_0 , τ_{total} , and NBW, the design procedure is summarized in the following steps.

Step 1: Initialize $\text{FBW} = 0.1$, $N = 2$, a with (12), $b = 0$ and the g_i of the corresponding low-pass prototype.

Step 2: Calculate Z_{oi} and Z_{ei} with (4), τ_{C1} with (11) and R_i with (7) and (8). Then, the first test value τ_{total1} of NGD is obtained. Set $\tau_{C2} = 0.9\tau_{C1}$ to obtain the second test value τ_{total2} of NGD.

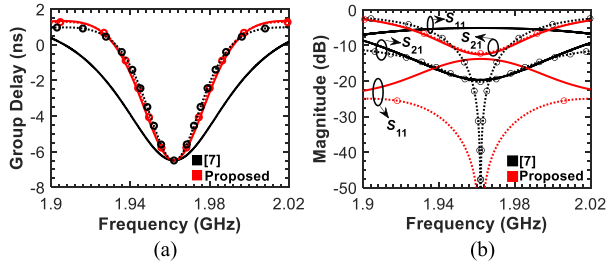


Fig. 5. Synthesized responses of the matched and unmatched third-order absorptive BSFs, compared to the filters in [7]. (a) Group delay and (b) magnitude, where the dashed lines with circles are for the matched cases, while the solid lines are for the unmatched cases.

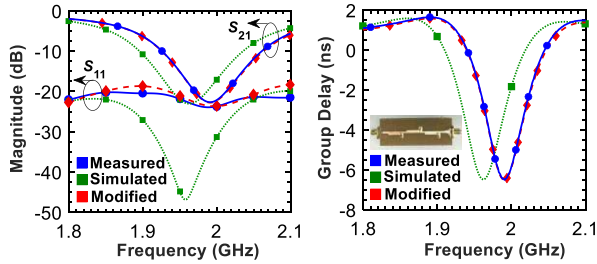


Fig. 6. Measured, simulated, and modified results of the proposed filter.

- Step 3: Update a and b by solving (11) with the two tests $[\tau_{C1}, \tau_{total1}]$ and $[\tau_{C2}, \tau_{total2}]$, and then obtain τ_C from (11).
- Step 4: Update R_i with (7) and (8), and obtain the achieved NBW. If the NBW is not equal to the prescribed one, scale FBW and go to Step 2.
- Step 5: If the final calculated FBW is unrealizable, go to Step 1 with $N = N + 1$.
- Step 6: Calculate Q_i with (2), set proper values of θ_{si} and Q_{i0} , and calculate R_{si} with (10).
- Step 7: Optimize the filter structure.

III. RESULTS AND DISCUSSION

A third-order BSF prototype is designed, with the prescribed $f_0 = 1.962$ GHz, NBW = 110 MHz, and $\tau_{total} = -6.5$ ns. The element values of low-pass prototype are $[g_0 \dots g_4] = [1, 0.6292, 0.9703, 0.6292, 1]$. The values of $\tau_C = -2.545$ ns, FBW = 13.5%, $[Z_{o1}, Z_{o2}, Z_{o3}] = [40.0, 38.3, 40.0] \Omega$, $[Z_{e1}, Z_{e2}, Z_{e3}] = [66.67, 71.99, 66.67] \Omega$, and $[R_1, R_2, R_3] = [576.9, 1768.8, 1942.1] \Omega$ are obtained by applying the above design steps. The desired Q -factor of each resonator is calculated by (2) to be $[Q_1, Q_2, Q_3] = [8.49, 25.19, 28.60]$. The prototype is fabricated on a 1-mm-thick FR4 substrate, with $\epsilon_r = 4.4$ and $\tan\delta = 0.02$, where the Q -factors of $\lambda/4$ resonators without resistor loading are about $Q_{i0} = 50$. Here, we choose $[R_{s1}, R_{s2}, R_{s3}] = [110, 620, 680] \Omega$, which are available in practice, and θ_{si} is about 0.42 rad from (10). To compensate for the difference between the odd- and even-mode electrical lengths of coupled microstrip line, the microstrip lines are decoupled near the shorted end [8]. The optimized structure and parameters are given in Fig. 3.

The simulated and measured S-parameters and NGDs of the prototype are shown in Fig. 6. Reasonable agreement is achieved between them. The measured response is centered at 1.99 GHz, and the frequency deviation of 28 MHz from the simulated one is mainly due to the tolerance of permittivity. The difference of RL between the measured and simulated results is mainly caused by the tolerances of resistor mounting and fabrication, especially the small gaps in the coupled

TABLE I
PERFORMANCE COMPARISON OF PROPOSED NGD
BSF WITH PREVIOUS WORKS

	Size $\lambda_g \times \lambda_g$	f_0 GHz	NGD ns	IL dB	RL dB	NBW MHz	NGD- NBW
[3]	$\approx 0.5 \times 0.5$	2.14	-7.9	16.5	-	60	0.474
[4]	0.50×0.30	2.14	-6.3	20.7	6	70	0.441
[5]	0.37×0.48	2.14	-1.0	3.8	12	60	0.060
[6]	0.78×0.06	1.0	-1.5	33	25	370	0.555
[7]	0.63×0.42	1.96	-6.5	21.2	9	81	0.527
Ours	0.76×0.16	1.99	-6.5	22.6	21	105	0.683
Syn	-	1.96	-6.5	21.8	20	110	0.715

λ_g : the guided wavelength of a 50- Ω microstrip line at f_0 ; **Syn**: the synthesized results of the proposed NGD BSF; and **RL**: the worst RL within the NGD band.

lines. The simulated result with slightly modified substrate $\epsilon_r = 4.28$ and geometric parameters $[L_{r12}, L_{r22}, L_{r32}, g_2] = [4.35, 3.7, 3.55, 0.33]$ mm is also shown in Fig. 6 for comparison.

The measured NGD is -6.5 ns, with the IL of 22.6 dB and the worst RL of 21 dB within the NGD band. Table I shows the performance comparison of the proposed BSF with the previous works. Our synthesized results agree well with the measured ones except that the IL is smaller as expected. Due to the first coupled-line section working as an absorptive matching network also with an NGD, the proposed filter shows improved RL (by 12 dB) and enhanced bandwidth (by 30%) for the NGD band, when the NGD is the same as that in [7]. The NGD-NBW product is better than the other circuits with comparable RL. Our circuit size is smaller than the previous ones except for [6].

IV. CONCLUSION

An absorptive BSF, based on coupled-line structures, has been designed with prescribed NGD and NBW. A set of resistors is loaded on the resonators so as to tune the Q -factors and match the BSF within its NGD band. The proposed method can be applied directly without further tuning the critical parameters in design. Good agreement is obtained between our simulated and measured results of the third-order filter prototype to demonstrate the proposed idea.

REFERENCES

- [1] Y. Jeong, H. Choi, and C. D. Kim, "Experimental verification for time advancement of negative group delay in RF electronics circuits," *Electron. Lett.*, vol. 46, no. 4, pp. 306–307, Feb. 2010.
- [2] M. Kadic and G. E. Bridges, "Limits of negative group delay phenomenon in linear causal media," *Prog. Electromagn. Res.*, vol. 134, pp. 227–246, 2013.
- [3] G. Chaudhary and Y. Jeong, "Distributed transmission line negative group delay circuit with improved signal attenuation," *IEEE Microw. Wireless Compon. Lett.*, vol. 24, no. 1, pp. 20–22, Jan. 2014.
- [4] G. Chaudhary and Y. Jeong, "Transmission-type negative group delay networks using coupled line doublet structure," *IET Microw. Antennas Propag.*, vol. 9, no. 8, pp. 748–754, Jun. 2015.
- [5] G. Chaudhary and Y. Jeong, "Negative group delay phenomenon analysis using finite unloaded quality factor resonators," *Prog. Electromagn. Res.*, vol. 156, pp. 55–64, 2016.
- [6] C.-T. M. Wu and T. Itoh, "Maximally flat negative group-delay circuit: A microwave transversal filter approach," *IEEE Trans. Microw. Theory Techn.*, vol. 62, no. 6, pp. 1330–1342, Jun. 2014.
- [7] G. Chaudhary, Y. Jeong, and J. Lim, "Microstrip line negative group delay filters for microwave circuits," *IEEE Trans. Microw. Theory Techn.*, vol. 62, no. 2, pp. 234–243, Feb. 2014.
- [8] J.-Y. Shao and Y.-S. Lin, "Narrowband coupled-line bandstop filter with absorptive stopband," *IEEE Trans. Microw. Theory Techn.*, vol. 63, no. 10, pp. 3469–3478, Oct. 2015.